THE JOURNAL OF PHYSICAL CHEMISTRY A

Article

pubs.acs.org/JPCA

# Heterogeneous Kinetics of *cis*-Pinonic Acid with Hydroxyl Radical under Different Environmental Conditions

Chengyue Lai, Yongchun Liu,* Jinzhu Ma, Qingxin Ma, Biwu Chu, and Hong He*

State Key Joint Laboratory of Environment Simulation and Pollution Control, Research Center for Eco-Environmental Sciences, Chinese Academy of Sciences, Beijing, 100085, China

Supporting Information

**ABSTRACT:** To understand the atmospheric fate of secondary organic aerosol (SOA), heterogeneous degradation behaviors of a specific tracer derived from α-pinene−*cis*-pinonic acid (CPA), initiated by hydroxyl radicals (OH), were investigated under different environmental conditions using a flow reactor. The second-order rate constant ($k_2$) of the CPA−OH reaction was determined to be $(6.17 \pm 1.07) \times 10^{-12}$ cm$^3$·molecule$^{-1}$·s$^{-1}$ at 25 °C and 40% relative humidity (RH). Higher temperature promoted this reaction, while relative humidity had a little inhibiting effect on it. The atmospheric lifetime of CPA varied from 2.1 to 3.3 days under different environmental conditions. Infrared spectrometry (IR), density functional theory (DFT) calculation and gas chromatography coupled mass spectrometry (GC−MS) results indicated that the oxidation products should be ascribed to poly(carboxylic acid)s. This study shows that the heterogeneous degradation of CPA initiated by OH radical is appreciable, and the concentrations of CPA measured in field measurements may underestimate the corresponding precursors of SOA.

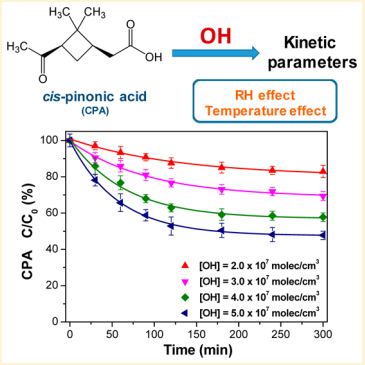


## 1. INTRODUCTION

Organic aerosols have been recognized to be significant constituents of fine particles, which contain numerous organic components derived from biogenic, anthropogenic and photochemical sources.[1] Secondary organic aerosol (SOA), which is formed through the gas phase oxidation of volatile organic compounds (VOCs) by atmospheric oxidants such as OH radicals, $NO_3$ radicals, and ozone, is a major fraction of organic aerosol loading in the atmosphere and has a prominent influence on human health, visibility degradation and climate change.[2−8] The oxidation process occurs by formation of semi- and low-volatile compounds followed by nucleation process and condensation onto pre-existing particles, or by direct heterogeneous reactions of VOCs and their gaseous oxidation products on particle surfaces.[9−12] VOCs of high atmospheric abundance and with high reactivity are expected to be the major precursors to SOA formation, which include gaseous biogenic emissions such as isoprene, monoterpenes, sesquiterpenes, and anthropogenic emissions of aromatic compounds and other solvents.[13−26]

α-Pinene is a major compound with globally high emission rates that can represent monoterpenes in the atmosphere.[27,28] *cis*-Pinic, *cis*-norpinic and *cis*-pinonic acid have been widely confirmed to be the primary products formed through the photooxidation of α-pinene with OH radicals and $O_3$.[29−34] These products are often regarded as α-pinene SOA tracers, which can be used to estimate the fraction of organic aerosol from α-pinene.[35] Among all the α-pinene SOA tracers, *cis*-pinonic acid (CPA, chemical structure shown in Figure 1) has the highest level, by a factor of 3 compared with other tracers.[12]

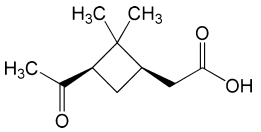

**Figure 1.** Chemical structure of *cis*-pinonic acid (CPA).

Specific SOA tracers can provide insight on precursors and processes influencing SOA production. Recently, a few studies have estimated the SOA sources based upon the ratio of the tracers to the corresponding SOA mass loading obtained through chamber experiments, as well as the detected concentrations of these tracers in ambient particles.[35−38] In this method, it is assumed that the SOA tracers are stable in the atmosphere, unique to their precursor gas, and formed only by secondary reactions.[38] However, field measurements have shown that the atmospheric concentrations of major SOA products (*cis*-pinonic acid and *cis*-pinic acid) from α-pinene are low during summer compared with other seasons. This indicates that these tracers undergo chemical degradation, from which highly oxygenated products may form through oxidation in the atmosphere.[32] This phenomenon has been further confirmed by many other researchers.[5,39−42] For instance, Szmigielski et al. have found that CPA can react with OH radicals in the presence of $NO_x$ and form a more stable $C_8$-tricarboxylic acid 3-methyl-1,2,3-butanetricarboxylic acid (MBTCA).[32] Müller et al. further confirmed the formation

**Received:** February 9, 2015
**Revised:** May 15, 2015
**Published:** May 28, 2015

ACS Publications © 2015 American Chemical Society



DOI: 10.1021/acs.jpca.5b01321
J. Phys. Chem. A 2015, 119, 6583−6593

of MBTCA via gas phase oxidation of CPA, and proposed several feasible radical mechanisms for the generation of MBTCA.[5] Using cyclobutyl methyl ketone as a model compound for CPA, Praplan et al. also found three probable products (MBTCA, terpenylic acid and diaterpenylic acid acetate) from OH oxidation of CPA in the gas phase.[40] Through such studies, when OH react with CPA in the gas phase, hydrogen abstraction will first occur, followed by the formation of alkoxy radicals and carbon−carbon bonds dissociation. Field measurements also discovered an obvious decay of CPA and other organic tracers during transport.[37] All of these previous laboratory studies mentioned above investigated the gas phase reactions between CPA and oxidants, which may because CPA is neither sufficiently nonvolatile nor hygroscopic.[43,44] The higher volatility compared to some of the other known SOA compounds (tracers) from $\alpha$-pinene oxidation will lead to the remove of *cis*-pinonic acid from the aerosol system and the production of other known SOA tracers in the gas phase. However, the CPA is a semivolatile organic compound with vapor pressure of $(0.5-1) \times 10^{-4}$ Pa.[45] Estimated with the partitioning model, 40.0% - 57.2% of CPA will present in particle phase at 296 K assuming 5 $\mu g \cdot m^{-3}$ of organic mass loading in the atmosphere.[46] This is well supported by the fact that CPA was frequently detected in particulate matter in the atmosphere.[5,47−49] Therefore, like other semivolatile compounds,[50−52] heterogeneous kinetics of CPA should also be important for the understanding its atmospheric lifetime, while it is unavailable yet at present time.

In this study, the heterogeneous degradation behaviors of particulate *cis*-pinonic acid initiated by OH radicals under different environmental conditions have been measured using a flow reactor. The kinetic parameters and atmospheric lifetime of CPA under different relative humidity and temperature were determined, and possible products for this reaction were also discussed. This study first reported the heterogeneous kinetics of CPA toward OH radical. It will be helpful for both understanding the lifetime of CPA and evaluating the rationality to use CPA as a SOA tracer.

## 2. EXPERIMENTAL SECTION

**2.1. Experimental Methods.** All the experiments were performed in a flow reactor, which contains a quartz tube irradiated with UV light for OH generation and a stainless steel reactor for dark reaction. The schematic diagram of the experimental setup used in this study is shown in Figure S1 (Supporting Information) and the details of the setup were described in our previous work.[53] For the kinetic studies, a dry film of $(10.0 \pm 0.1)$ $\mu$g CPA was placed on a disk, which was evenly generated by gently drying a CPA/methanol solution with $N_2$ flow. Although the CPA in this study was presented in film form instead of suspended particles, our previous study has confirmed the feasibility of this method in the investigation of the degradation kinetics of levoglucosan.[53]

The reactions between CPA and OH radicals were carried out in air flow with a constant OH concentration. The total flow rate was 500 $mL \cdot min^{-1}$ with simulated air (80% high purity $N_2$ and 20% high purity $O_2$) and bubbled $H_2O_2$ flow. The RH of the system was controlled by varying the ratio of wet $N_2$ flow, which was achieved by bubbling nitrogen through $H_2O$, to dry $N_2$ flow, and was determined by a humidity temperature meter (CENTER-314) at the exit of the reactor. The temperature of the system was controlled by a circulating water bath (CCA-20, Gongyi City YUHUA Instrument Co., Ltd.) with uncertainty less than 0.5 °C. The water partial pressure in the system may change when the temperature changes, but the RH in the reactor can be maintained at different temperatures by adjusting the ratio of wet $N_2$ flow to dry $N_2$ flow. Since direct irradiation of the samples by UV light was avoided (as shown in Figure S1), any decay of reactants should result from oxidation by OH radicals in the dark.

Reacted samples were ultrasonically extracted using $(20.0 \pm 0.1)$ mL methanol and then filtered using a glass fiber filter that had been previously cleaned by methanol. The eluate was evaporated to near dryness, and subsequently transferred into a 1.5 mL sealed vial, then dried to residue under a gentle nitrogen stream.

Because of the high polarity of CPA, a derivatization step is required prior to GC analysis, and silylation is recognized as the best derivatization method to reduce the polarity.[54] Detailed derivatization steps and GC−MS parameters are shown in the Supporting Information. The concentration of CPA was measured based on an external standard and the use of a calibration curve. Moreover, the recovery of CPA varied from 96.8% to 109.4%, demonstrating that this analytical method was suitable for the determination of CPA and repeated experiments were carried out to minimize the experimental uncertainty.

**2.2. OH Generation and Detection.** The OH radicals were generated in a quartz tube by UV photolysis of $H_2O_2$. Two ultraviolet light lamps (18 W, Beijing Lighting Research Institute) that provided UV-radiation with a central wavelength around 254 nm were used. The concentration of OH radical was controlled by varying the ratio of pure $N_2$ and $H_2O_2$ flow passing through the tube.

Salicylic acid (SA) has strong reactivity with OH radical, and thus has commonly been used to trap OH radicals.[55] In this study, the yields of the products (2,3-dihydroxybenzonic acid and 2,5-dihydroxybenzonic acid) during the reactions between salicylic acid and OH were used to estimate the concentration of near-surface OH radicals. Detailed descriptions of the experimental procedures for OH determination are shown in the Supporting Information. This method has usually been used for liquid phase OH determination and has been verified in our previous work, as the measured $k_2$ of levoglucosan toward hydroxyl radical is comparable with literature values.[53,56] When the experiment for OH determination was carried out, salicylic acid (not mixed with CPA) was placed on the Teflon disk at the same position as for CPA, and the experimental conditions for OH oxidation were the same as that for CPA oxidation. The OH concentration were adjusted from $2 \times 10^7$ to $5 \times 10^7$ $molecule \cdot cm^{-3}$ for subsequent experiments. Furthermore, seven repeat experiments were carried out for each OH concentration. The relative standard deviations (RSD) of OH concentration were less than 10%.

**2.3. Characterization of CPA and Its Oxidation Products.** The functional groups of the samples were characterized using a Fourier transform infrared spectrometer (FT-IR, NEXUS 6700, Thermo Nicolet Instrument Corp.) equipped with a high-sensitivity mercury−cadmium-telluride (MCT) detector cooled by liquid $N_2$ and an ATR-IR cell. The spectra of the samples were recorded (100 scans, 4 $cm^{-1}$ resolution) using the blank ZnSe crystal as reference.

The gas chromatography (7890B, Agilent Technologies) coupled mass spectrometry (5977A, Agilent Technologies) (GC−MS) in scan mode was also used to idetify the possible products. The capillary column HP-5MS (30 m, 0.25 mm


DOI: 10.1021/acs.jpca.5b01321
J. Phys. Chem. A 2015, 119, 6583−6593

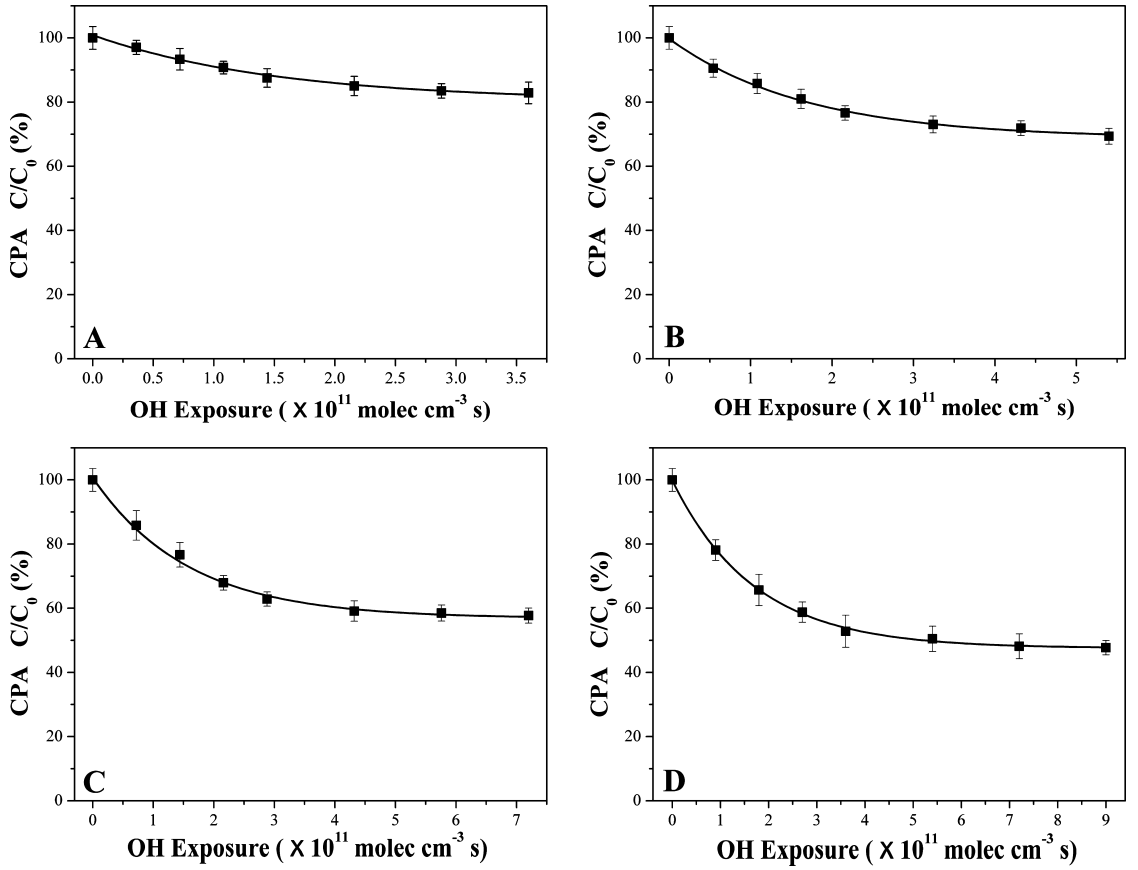


**Figure 2.** Representative decay curves for *cis*-pinonic acid (CPA) under different OH concentrations at 25 °C and 40% RH as a function of OH exposure ($n$ = 3, error bars represent one standard deviation based on triplicate analyses). (A) [OH] = 2.0 × $10^7$ molecules·$cm^{-3}$; (B) [OH] = 3.0 × $10^7$ molecules·$cm^{-3}$; (C) [OH] = 4.0 × $10^7$ molecules·$cm^{-3}$; (D) [OH] = 5.0 × $10^7$ molecules·$cm^{-3}$. Samples were exposed to OH radicals from 0 to 300 min (0, 30, 60, 90, 120, 180, 240, and 300 min for each point, respectively).

internal diameter, 0.25 $\mu$m film thickness) was installed in the GC and its output was inserted directly into the ion source of the MS. Each sample was introduced via EPC splitless mode injection. The oven temperature was held at 50 °C for 5 min, then programmed to 200 °C at a ramp of 3 °C·$min^{-1}$ and held at 200 °C for 2 min, finally programmed to 300 °C at a ramp of 30 °C·$min^{-1}$. Helium was used as carrier gas at a constant flow rate of 1.0 mL·$min^{-1}$. The temperatures of the injector and transfer line were 250 and 280 °C, respectively. The mass detection was performed between $m/z$'s 50−650.

Moreover, the Gaussian 09 suite of programs was also used to assign the vibrational model of CPA and its oxidation products.[57] Geometry optimizations and vibrational frequency calculations were performed at the mpw1pw91 DFT level of theory with 6-311+g(d,p) basis set. The calculated frequency was scaled by 0.958.[58]

**2.4. Chemicals.** All the chemicals were of chromatographic grade and used as received. Methanol was obtained from Fisher Scientific. *cis*-Pinonic acid (98.0%) was purchased from Sigma-Aldrich. *N,O*-Bis(trimethylsilyl)trifluoroacetamide plus trimethylchlorosilane (BSTFA:TMCS = 99:1) and salicylic acid (>99.5%) were purchased from Tokyo Chemical Industry Co., Ltd. Pyridine and 30% $H_2O_2$ were purchased from Sinopharm Chemical Reagent Co. High purity $N_2$ (99.99%) and $O_2$ (99.99%) were supplied by Beijing HUAYUAN Gases Inc.

## 3. RESULTS AND DISCUSSION

**3.1. Kinetic Measurements for *cis*-Pinonic Acid−OH Reaction.** In order to evaluate the influence of vaporization and degradation by $H_2O_2$ on *cis*-pinonic acid, blank experiments were performed under the same air flow and $H_2O_2$ flow as those in the OH oxidation experiments at different temperatures. The experiments were carried out at 40% RH in the dark. The results are shown in Figure S2, from which indicate that the decrease in the amount of pure *cis*-pinonic acid was lower than 10% at both 5 and 35 °C over 5 h purging regardless of the carrier gas, and that $H_2O_2$ does not react with CPA. As the experiments in this study were all carried out in the temperature range between 5 and 35 °C, the slight decrease of CPA concentration due to evaporation will not have much influence on the CPA−OH reaction. The evaporation effect has been considered in the kinetics interpretation.

To accurately determine the rate constant of the CPA−OH reaction, CPA was oxidized under four different OH concentrations (near-surface gas phase concentration, similarly hereinafter), which were estimated by the degradation experiments of salicylic acid separately as previously mentioned. The OH concentrations used in this part were 2.0 × $10^7$, 3.0 × $10^7$, 4.0 × $10^7$, and 5.0 × $10^7$ molecules·$cm^{-3}$, respectively.

The kinetic data were determined by monitoring the loss of CPA concentration as a function of OH exposure at 25 °C with 40% RH in the dark. Assuming a second-order reaction between OH and CPA, the loss rate of CPA can be expressed as follows:


DOI: 10.1021/acs.jpca.5b01321
J. Phys. Chem. A 2015, 119, 6583−6593

**Table 1. Calculated Rate Constant and Atmospheric Lifetime of *cis*-Pinonic Acid (CPA) for the Reaction between *cis*-Pinonic Acid and OH Radical under Different Atmospheric Conditions**

| reaction conditions | | | second-order rate constant ($k_2$, $cm^3 \cdot molecule^{-1} \cdot s^{-1}$) | atmospheric lifetime (days)[a] |
|---|---|---|---|---|
| reactions under different OH concentrations | OH concentration ($molecule \cdot cm^{-3}$)[b] | $2.0 \times 10^7$ | $(6.48 \pm 0.76) \times 10^{-12}$ | – |
| | | $3.0 \times 10^7$ | $(5.99 \pm 0.46) \times 10^{-12}$ | – |
| | | $4.0 \times 10^7$ | $(6.33 \pm 0.40) \times 10^{-12}$ | – |
| | | $5.0 \times 10^7$ | $(5.86 \pm 0.14) \times 10^{-12}$ | – |
| | | **average** | $\mathbf{(6.17 \pm 1.07) \times 10^{-12}}$ | **2.3 ± 0.3** |
| RH effect[c] | | 20% RH | $(6.48 \pm 0.17) \times 10^{-12}$ | 2.2 ± 0.1 |
| | | 40% RH | $(6.33 \pm 0.40) \times 10^{-12}$ | 2.3 ± 0.2 |
| | | 60% RH | $(5.62 \pm 0.48) \times 10^{-12}$ | 2.6 ± 0.2 |
| | | 80% RH | $(5.40 \pm 0.22) \times 10^{-12}$ | 2.7 ± 0.1 |
| temperature effect[d] | | 5 °C | $(4.39 \pm 0.31) \times 10^{-12}$ | 3.3 ± 0.3 |
| | | 15 °C | $(5.11 \pm 0.16) \times 10^{-12}$ | 2.8 ± 0.1 |
| | | 25 °C | $(6.33 \pm 0.40) \times 10^{-12}$ | 2.3 ± 0.2 |
| | | 35 °C | $(6.85 \pm 0.27) \times 10^{-12}$ | 2.1 ± 0.1 |

[a]Assuming the typical concentration for 12 h average value of OH to be $1.6 \times 10^6$ molecules·$cm^{-3}$. [b]Experimental condition: RH = 40%. Temperature = 25 °C. [c]Experimental condition: [OH] = $4.0 \times 10^7$ molecules·$cm^{-3}$. Temperature = 25 °C. [d]Experimental condition: [OH] = $4.0 \times 10^7$ molecules·$cm^{-3}$. RH = 40%.

$$-\frac{d[CPA]}{dt} = k_2[OH][CPA] \quad (1)$$

where [OH] is the near-surface OH concentration (molecules·$cm^{-3}$), [CPA] is the concentration of *cis*-pinonic acid and $k_2$ is the second-order rate constant for the reactions between CPA and OH. Since the OH concentration is constant during the experimental procedure, eq 1 can be integrated from zero to the residence time ($t$) of reactants:

$$\ln \frac{[CPA]}{[CPA]_0} = -k_2[OH]t \quad (2)$$

where $[CPA]_0$ is the initial concentration of *cis*-pinonic acid.

Figure 2 shows the changes in $[CPA]/[CPA]_0$ as a function of OH exposure under different OH concentrations at 40% RH and 25 °C. The lines are the exponential curve fitting ($y = y_0 + e^{-x/t}$) results. From the fitting process, two fitted parameters ($y_0$ and $t$) can be obtained. Deduced from eq 2, the second-order rate constant can be derived through parameter $t$ ($k_2 = 1/t$). The calculated $k_2$ values under different OH concentrations are listed in Table 1. A plateau can be observed in the degradation curve of CPA because CPA cannot be consumed completely even under high OH exposure. This plateau might result from the diffusion limit of OH in the solid phase and the influence of oxidation products remaining on the surface, which has been widely observed in other reaction systems.[59,60] The decrease of the CPA fraction remaining (at the plateau) with increased OH concentration was probably due to more OH radicals diffusing into CPA in the beginning of the reaction after some oxidation products are further oxidized to small molecules with high vapor pressure, which may deplete the CPA on the surface for further OH reaction under higher OH concentrations.

Both external (gaseous reactants from gas phase to the surface) and internal diffusion (from the surface layer to the underlying layers and into the pores of particles or films) should be considered when a heterogeneous reaction is carried out under ambient pressure and on packed powder samples if a gas phase reference is utilized to measure gas phase OH concentration.[61−63] However, as discussed in our previous work and in the Supporting Information,[53] both external and internal diffusion corrections are unnecessary in this study because the near-surface OH concentrations instead of gas phase OH concentrations were measured through utilization of a particle phase reference, and all the samples used in this work are nonporous with smooth surfaces (shown in Figure S3). Moreover, the reactions between OH and organic compounds are recognized to be limited to the surface.[64]

At 25 °C, the $k_2$ values (shown in Table 1) for the CPA−OH reaction under different OH concentrations were comparable within the experimental uncertainty, with an average value of $(6.17 \pm 1.07) \times 10^{-12}$ $cm^3 \cdot molecule^{-1} \cdot s^{-1}$. This means the experiments are controllable and repeatable. At present, the experimental kinetics for the reaction between CPA and OH are unavailable. Using the Atmospheric Oxidation Program for Microsoft Windows (AOPWIN) based on the structure−activity relationship (SAR) methods developed by Atkinson et al., the $k_2$ value of the CPA−OH reaction was estimated to be $3.32 \times 10^{-12}$ $cm^3 \cdot molecule^{-1} \cdot s^{-1}$,[65,66] which is close to the results obtained from this work. On the other hand, based on the quantum chemical calculations at the B3LYP-DFT/6-31G(d,p) level of theory as implemented in the Gaussian 98 quantum chemical program, Vereecken et al. defined several reaction sites and calculated the hydrogen abstraction rate coefficients by OH at 6 different sites, with the total rate constant to be $1.04 \times 10^{-11}$ $cm^3 \cdot molecule^{-1} \cdot s^{-1}$,[67] and found that the hydrogen abstraction should dominantly occurs on the cyclobutyl ring. It should be pointed out that both SAR models and quantum chemical calculations are suitable for the gas phase reaction, which is different from the heterogeneous reactions in this study. Moreover, the uncertainties from quantum calculation or SAR model may also cause the diversity of the results between the theoretical and laboratory results. These factors may explain the disagreement between calculated $k_2$ values and the experimental data obtained in this study.

**3.2. Effect of Temperature.** The temperature of the system was regulated to 5, 15, 25, and 35 °C at a constant RH of 40% to investigate the effect of different temperatures on the CPA−OH reaction. The concentration of OH radical was adjusted to $4.0 \times 10^7$ molecules·$cm^{-3}$ and all the experiments were conducted in the dark. The changes in $[CPA]/[CPA]_0$ as



DOI: 10.1021/acs.jpca.5b01321
J. Phys. Chem. A 2015, 119, 6583−6593

a function of OH exposure at different temperatures at 40% RH are shown in Figure 3. Calculated $k_2$ values for CPA−OH reactions obtained through eq 2 are listed in Table 1.

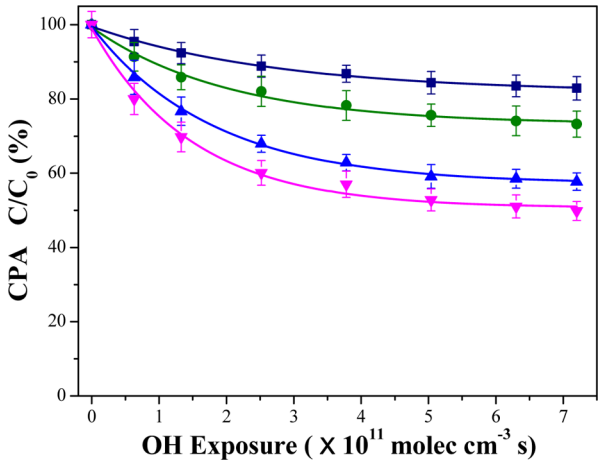


**Figure 3.** Representative decay curves for *cis*-pinonic acid (CPA) at different temperatures with a constant relative humidity of 40% as a function of OH exposure (■, 5 °C; ●, 15 °C; ▲, 25 °C; ▼, 35 °C; $n$ = 3, error bars represent 1 standard deviation based on triplicate analyses).

The results show that the degradation of CPA was significantly influenced by temperature. The calculated $k_2$ values increased from $(4.39 \pm 0.31) \times 10^{-12}$ $cm^3 \cdot molecule^{-1} \cdot s^{-1}$ at 5 °C to $(6.85 \pm 0.27) \times 10^{-12}$ $cm^3 \cdot molecule^{-1} \cdot s^{-1}$ at 35 °C. Figure 4 shows the Arrhenius plot of the measured rate

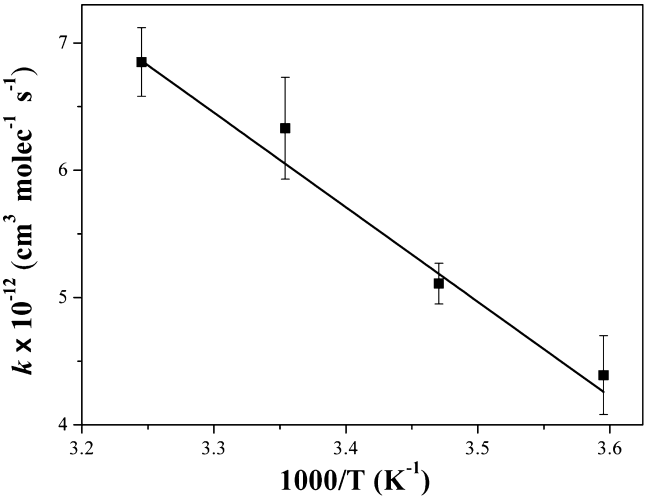


**Figure 4.** Measured rate constants for the reaction between *cis*-pinonic acid (CPA) and OH radical as a function of temperature.

constants for the reaction between CPA and OH, and the Arrhenius expression is expressed as $k_2=(3.2 \pm 4.8) \times 10^{-9}$ $\exp[(-1732.7 \pm 335.3)/T]$ in units of $cm^3 \cdot molecule^{-1} \cdot s^{-1}$. A positive temperature dependence was observed for this reaction and the overall activation energy was calculated to be $14.4 \pm 2.8$ $kJ \cdot mol^{-1}$. Previous works have found that temperature can either positively or negatively affect the reactions between different organic compounds and OH radicals.[68,69] In our previous study, which focused on the heterogeneous OH oxidation of levoglucosan and dehydroabietic acid, the overall activation energy were calculated to be $16.0 \pm 2.2$ and $12.5 \pm 0.5$ $kJ \cdot mol^{-1}$, respectively.[53] All the results show the positive temperature dependence of the rate constant, which means there is an activation energy for the formation of the transition state and that the reactivity is promoted by higher temperature, and these reactions readily proceed under ambient temperatures. In a work that focused on the gas phase oxidation of pinonic acid,[5] a positive temperature dependence was also found for the formation of MBTCA (3-methyl-1,2,3-butanetricarboxylic acid, an oxidation product of pinonic acid), which means the oxidation reaction of pinonic acid by OH may also be facilitated by higher temperature. Moreover, other investigations (including field measurements and laboratory studies) have found some biomass burning tracers, such as levoglucosan, to be more active with OH radical at higher temperatures.[53,70,71] As the degradation reactions of these tracers show positive temperature dependence, it is important to pay more attention to seasonal factors when investigating the aging process of such tracers.

**3.3. Effect of Relative Humidity.** To investigate the effect of different levels of relative humidity (RH) on the reactions between CPA and OH, the RH of the test system was adjusted to 20%, 40%, 60%, and 80% under a constant temperature of 25 °C. The concentration of OH radical was adjusted to approximately $4.0 \times 10^7$ $molecules \cdot cm^{-3}$ and all the experiments were carried out in the dark. The changes in $[CPA]/[CPA]_0$ as a function of OH exposure under different RH at 25 °C are shown in Figure 5. The $k_2$ values for CPA−OH

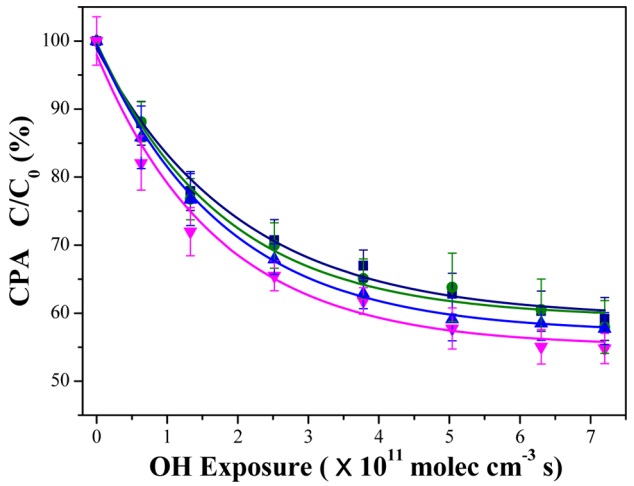


**Figure 5.** Representative decay curves for *cis*-pinonic acid (CPA) for different levels of relative humidity with a constant temperature of 25 °C as a function of OH exposure (■, 80% RH; ●, 60% RH; ▲, 40% RH; ▼, 20% RH; $n$ = 3, error bars represent 1 standard deviation based on triplicate analyses).

reactions calculated by eq 2 are also listed in Table 1. The results indicated that CPA degraded faster under lower relative humidity when temperature was fixed. The second-order rate constant linearly decreased with increasing RH, namely $k_2 = (6.86 \pm 0.10) \times 10^{-12} - (1.83 \pm 0.19) \times 10^{-12}$ $RH$ in units of $cm^3 \cdot molecule^{-1} \cdot s^{-1}$ ($r$ = 0.9681).

The water adsorption behavior of CPA was investigated using an AUTOSORB-1-C physisorption analyzer (Quantachrome, USA) to understand the influence of RH on the reactivity. The detailed methodology for the analysis method has been described elsewhere.[72] As shown in Figure 6, a slow


DOI: 10.1021/acs.jpca.5b01321
J. Phys. Chem. A 2015, 119, 6583−6593

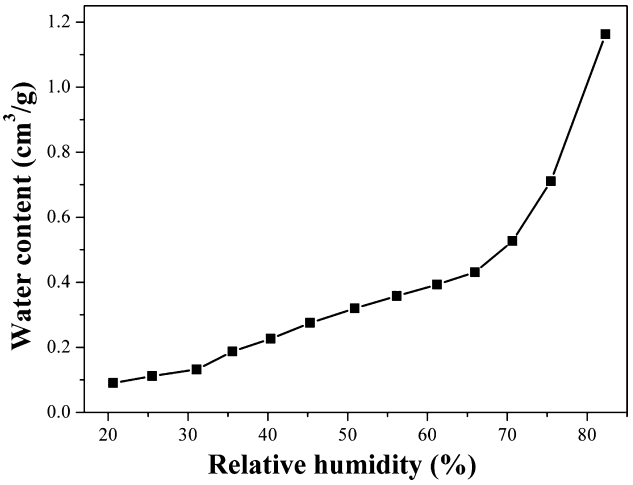


**Figure 6.** Adsorption isotherms of water on 149.5 mg *cis*-pinonic acid (CPA) at RH 20−80%.

increase rate of water adsorption can be observed in the range 20−80% RH. Through two-parameter BET equation fitting, monolayer adsorption of water was found to occur at 45.6% RH on CPA, which means there are less than two layers of water adsorbed on the surface of CPA in the RH region 20−80%. It has been found that relative humidity can either positively or negatively influence reactions between OH and the organic particles. Some researchers have observed that increased RH will lower the viscosity of the amorphous aerosol particles and subsequently enhance the OH uptake because particle-phase diffusion is feasible,[52,73,74] while some other results show that the OH uptake was suppressed at higher RH due to the competitive coadsorption of water, which will take up the reactive sites.[75] As for this study, since the solubility of CPA in water is low, the water molecules adsorbed on the surface of CPA under 20−80% RH may be not enough to soften CPA, but could occupy the reactive sites for OH radicals. Therefore, the water layers accumulated on the surface may decrease the reactivity of CPA, as the diffusion of OH may be inhibited due to limited OH radical transfer to the reaction site. The results obtained from this work are similar to those in recent studies carried out on OH oxidation of another proposed secondary organic aerosol tracer—methylnitrocatechol,[75] which means the RH effect is still noteworthy in the aging process of SOA tracers.

**3.4. Product Inference for *cis*-Pinonic Acid−OH Reaction.** Figure 7 shows IR spectra of CPA and its products after 30, 120, and 240 min of reaction with OH radicals at 25 °C and 40% RH, respectively. The characteristic absorption peaks and functional groups are assigned based upon both previous research and DFT calculations, and are given in Table 2. As can be seen in Figure 7, the absorption peaks of the alicyclic (cyclobutyl) group (1257, 1096, 1028, and 803 cm$^{-1}$)[76] decreased dramatically after reaction with OH, indicating the quaternary alicyclic structure of CPA was changed after the reaction. The absorption peaks of methylene groups (2921, 2852 cm$^{-1}$)[77,78] and methyl groups (1460, 1417, 1374, and 2954 cm$^{-1}$)[77,79] also decreased after a period of reaction, which means alkyl groups in CPA molecules were consumed. Moreover, the absorption peaks of carboxyl groups (1557, 1575 cm$^{-1}$)[80] increased slightly after the reaction. As CPA contains only one carboxyl group, it can be inferred that the product may contain more carboxyl groups. In conclusion, it can be inferred that the priority reaction site of CPA toward

**Table 2. Functional Groups Observed for *cis*-Pinonic Acid (CPA) and Its Products after Reaction with OH Radicals**

| peak, cm$^{-1}$ | functional group | DFT estimation peak,[a] cm$^{-1}$ |
|---|---|---|
| 2954 | alkane $CH_3$ stretch[77] | 2954 |
| 2921, 2852 | alkane $CH_2$ stretch[77,78] | 2915, 2852 |
| 1557 (1575) | —COOH asymmetric stretch[80] | – |
| 1460, 1417, 1374 | alkane $CH_3$ bending[79] | 1443, 1411, 1368 |
| 1257 | alicyclic (cyclobutyl, C−C) group | 1235 |
| 1096, 1028, 803 | alicyclic (cyclobutyl, C−H) group[76] | 1108, 987, 818 |

[a]The calculated frequency was scaled by 0.958.[58]

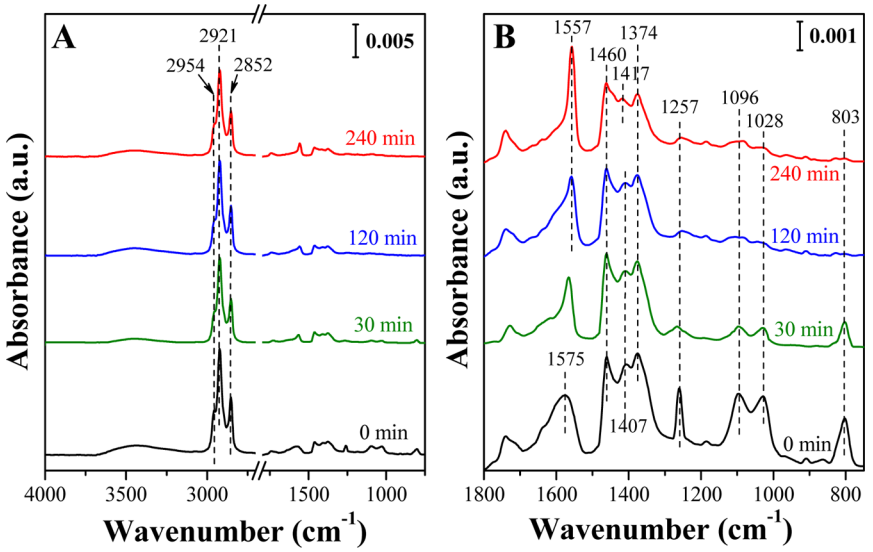


**Figure 7.** Normalized ATR-IR spectra for *cis*-pinonic acid (CPA) and its products after reaction with OH radicals. (A) Spectra in the wavenumber range between 4000 and 750 cm$^{-1}$. (B) Spectra in the wavenumber range between 1800 and 750 cm$^{-1}$.



DOI: 10.1021/acs.jpca.5b01321
J. Phys. Chem. A 2015, 119, 6583−6593

OH should be the H atom on the cyclobutyl group, and the H-abstraction will occur first in the reaction process. After a period of reaction, the alicyclic ring of CPA opens and the terminal methyl group is oxidized to a carboxyl group, resulting in poly(carboxylic acid)s.

To determine the potential products for the reaction, the GC−MS analysis in scan mode was carried out. To better compare with the literature results, levoglucosan was chosen to be the internal standard compound. Figure 8A and Figure 9A

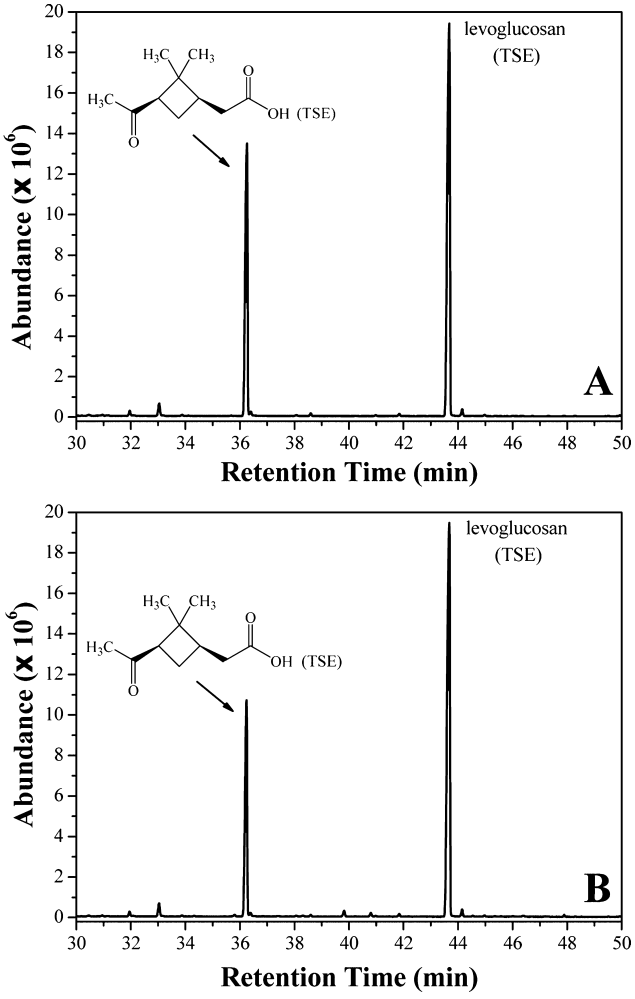


**Figure 8.** GC−MS total ion chromatogram (TIC) for the trimethylsilylation ester (TSE) of *cis*-pinonic acid and its OH oxidation products. (A) initial TIC for *cis*-pinonic acid trimethylsilylation ester (retention time 36.20 min); (B) trimethylsilylation ester of *cis*-pinonic acid and its oxidation products after 4 h reaction with OH.

show the initial TIC of *cis*-pinonic acid trimethylsilylation ester (TSE, with added levoglucosan), and Figure 8B and Figure 9B show the TIC of *cis*-pinonic acid and its oxidation products (trimethylsilylation ester) after 4 h reaction with OH. After 4 h reaction, the intensity of *cis*-pinonic acid (retention time 36.20 min) decreased. At the same time, some small peaks appeared (shown in Figure 9). Through NIST database, these small peaks cannot be well fitted due to their low intensity, the interference from column bleeding and derivation reaction. However, a previous study has simultaneously identified MBTCA and levoglucosan using the same type of chromatographic column and the same analysis procedure as used in this study.[81] They reported the retention time of MBTCA and

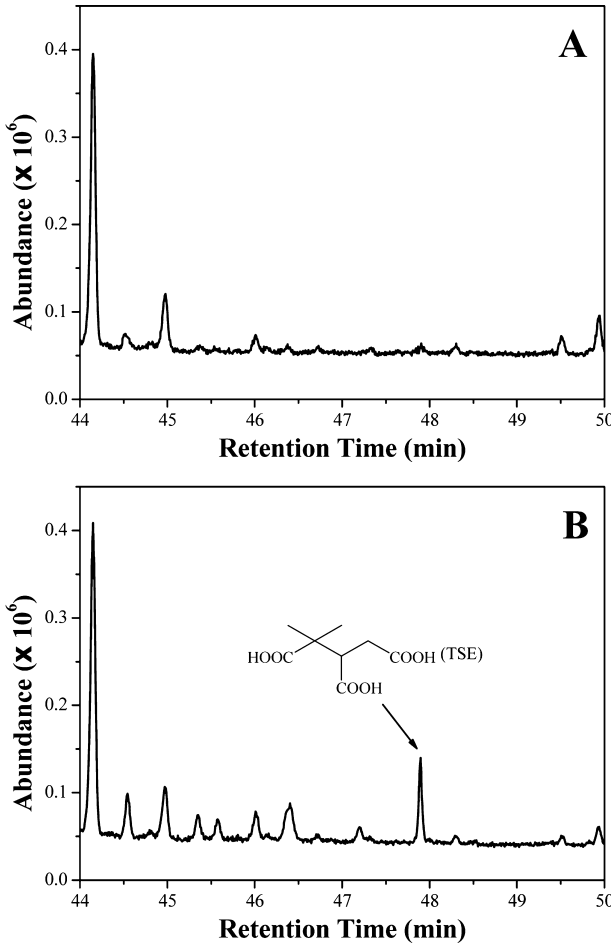


**Figure 9.** Magnified GC−MS total ion chromatogram (TIC) for the trimethylsilylation ester (TSE) of *cis*-pinonic acid and its OH oxidation products: (A) initial TIC; (B) trimethylsilylation ester of *cis*-pinonic acid oxidation products after 4 h reaction with OH.

levoglucosan to be 43.40 and 47.70 min, respectively. In our work, the retention time of levoglucosan is 43.68 min and is almost the same as that in the literature. The observed new peak with retention time at 47.90 min in this study is very close to MBTCA identified in their work. This peak has also been confirmed by the MS spectra at $m/z$ = 285. Therefore, the peak at retention time 47.90 min can be ascribed to MBTCA in Figure 9B. This result can confirm the interpretation of the IR results in regards to MBTCA.

In previous studies, MBTCA, terpenylic acid and diaterpenylic acid acetate have been suggested to be the gas phase OH oxidation products of CPA.[5,32,40] The IR results obtained in this study show that the CPA oxidation products from heterogeneous reaction can be attributed to the same category compared to the gas-phase reaction as MBTCA. However, as discussed in previous studies, although MBTCA has been recognized to be a product of CPA oxidation, its yield rate was less than 1%.[5] Therefore, more products still need be detected in future studies for more fully understand of CPA oxidation.

## 4. CONCLUSIONS AND ATMOSPHERIC IMPLICATIONS

In this study, the heterogeneous degradation behavior of CPA by OH radicals has been investigated using a flow reactor under different environmental conditions to evaluate the atmospheric stability of CPA. When exposed to OH radicals, a noteworthy



DOI: 10.1021/acs.jpca.5b01321
J. Phys. Chem. A 2015, 119, 6583−6593

degradation of CPA can be observed. Temperature plays an important role in the degradation rate of CPA, while relative humidity only has a small effect. In this study, the second-order rate constant ($k_2$) for the reaction of pure CPA in the particulate phase with OH was measured to be $(6.17 \pm 1.07) \times 10^{-12}$ $cm^3 \cdot molecule^{-1} \cdot s^{-1}$ at 25 °C and 40% RH. The $k_2$ of CPA increased with increasing temperature as expressed by the Arrhenius equation $k_2=(3.2 \pm 4.8) \times 10^{-9} \exp[(-1732.7 \pm 335.3)/T]$ at 40% RH, while it slightly decreased with increasing RH as expressed by $k_2 = (6.86 \pm 0.10) \times 10^{-12} - (1.83 \pm 0.19) \times 10^{-12}$ RH at 25 °C. ATR-IR results show that the cyclobutyl group of CPA opens during its reaction with OH, and the terminal methyl is oxidized to a carboxyl group, leading to poly(carboxylic acid)s.

OH, $NO_3$, and Cl radicals and $O_3$ are the main effective oxidants in the atmosphere, among which OH is considered to be the most dominant during daytime for organics.[82,83] Therefore, the rate coefficients obtained in this study can be used to estimate the atmospheric lifetime ($\tau$) of CPA, which was calculated according to the following equation:

$$\tau = \frac{1}{k_2[\mathrm{OH}]} \quad (3)$$

Assuming a 12 h average OH concentration to be $1.6 \times 10^6$ molecules·$cm^{-3}$ during daytime (25 °C and 101 kPa),[84,85] the atmospheric lifetime of pure CPA in the particle phase was calculated to be 2.3 ± 0.3 days. Under different environmental conditions, the lifetime, which is dependent on temperature and relative humidity, varied from 2.1 to 3.3 days.

It should be pointed out that the longest lifetime of CPA measured in this study is still shorter than the residence time of aerosols in the troposphere. Moreover, a recent study carried out by Tkacik er al. based on a tunnel experiment indicated that the peak SOA formation will occur after 2−3 days of atmospheric oxidation.[86] This means the concentration of CPA measured in field measurements may be underestimated for both atmospheric residence and SOA formation processes, which may cause the underestimation of corresponding precursors of SOA. Using the kinetic data obtained in this study may help to amend the field measurement data, and thus obtain more precise estimation results. Since the product of the CPA−OH reaction is still not clear enough among all the present studies, further research is needed to complete the list of the products. Furthermore, it has been found that mixing states play important roles in the chemical reactivity of organic aerosols.[87,88] In this study, the pure CPA samples only simulated the simplest case in the real atmosphere. The influence of mixing states of CPA with both inorganic species and soluble organic species on the reactivity should be further investigated and considered in the future.

## ■ ASSOCIATED CONTENT

### Supporting Information

Detailed experimental procedures for GC−MS analysis and OH determination, discussions about the diffusion corrections, and some figures showing a schematic diagram of the experimental set-up, the vaporization study of CPA in air flow, and SEM images. The Supporting Information is available free of charge on the ACS Publications website at DOI: 10.1021/acs.jpca.5b01321.

## ■ AUTHOR INFORMATION


### Corresponding Authors

*(Y.L.) Telephone: +86-10-62849337. E-mail: ycliu@rcees.ac.cn.

*(H.H.). Telephone: +86-10-62849123. E-mail: honghe@rcees.ac.cn.


### Notes

The authors declare no competing financial interest.

## ■ ACKNOWLEDGMENTS

This research was supported by the National Natural Science Foundation of China (21190054, 51221892) and the Strategic Priority Research Program of the Chinese Academy of Sciences (XDB05010300).

## ■ REFERENCES


(1) Kanakidou, M.; Seinfeld, J. H.; Pandis, S. N.; Barnes, I.; Dentener, F. J.; Facchini, M. C.; Van Dingenen, R.; Ervens, B.; Nenes, A.; Nielsen, C. J.; et al. Organic Aerosol and Global Climate Modelling: A Review. *Atmos. Chem. Phys.* **2005**, *5*, 1053−1123.

(2) Ziemann, P. J.; Atkinson, R. Kinetics, Products, and Mechanisms of Secondary Organic Aerosol Formation. *Chem. Soc. Rev.* **2012**, *41*, 6582−6605.

(3) Huang, R.-J.; Zhang, Y.; Bozzetti, C.; Ho, K.-F.; Cao, J.-J.; Han, Y.; Daellenbach, K. R.; Slowik, J. G.; Platt, S. M.; Canonaco, F.; et al. High Secondary Aerosol Contribution to Particulate Pollution During Haze Events in China. *Nature* **2014**, *514*, 218−222.

(4) De Gouw, J. A.; Middlebrook, A. M.; Warneke, C.; Goldan, P. D.; Kuster, W. C.; Roberts, J. M.; Fehsenfeld, F. C.; Worsnop, D. R.; Canagaratna, M. R.; Pszenny, A. A. P., et al. Budget of Organic Carbon in a Polluted Atmosphere: Results from the New England Air Quality Study in 2002. *J. Geophys. Res.* **2005**, *110*.

(5) Müller, L.; Reinnig, M. C.; Naumann, K. H.; Saathoff, H.; Mentel, T. F.; Donahue, N. M.; Hoffmann, T. Formation of 3-Methyl-1,2,3-Butanetricarboxylic Acid Via Gas Phase Oxidation of Pinonic Acid − a Mass Spectrometric Study of SOA Aging. *Atmos. Chem. Phys.* **2012**, *12*, 1483−1496.

(6) Maksymiuk, C. S.; Gayahtri, C.; Gil, R. R.; Donahue, N. M. Secondary Organic Aerosol Formation from Multiphase Oxidation of Limonene by Ozone: Mechanistic Constraints Via Two-Dimensional Heteronuclear NMR Spectroscopy. *Phys. Chem. Chem. Phys.* **2009**, *11*, 7810−7818.

(7) Donahue, N. M.; Tischuk, J. E.; Marquis, B. J.; Huff Hartz, K. E. Secondary Organic Aerosol from Limona Ketone: Insights into Terpene Ozonolysis Via Synthesis of Key Intermediates. *Phys. Chem. Chem. Phys.* **2007**, *9*, 2991−2998.

(8) Chu, B.; Liu, Y.; Li, J.; Takekawa, H.; Liggio, J.; Li, S. M.; Jiang, J.; Hao, J.; He, H. Decreasing Effect and Mechanism of $FeSO_4$ Seed Particles on Secondary Organic Aerosol in α-Pinene Photooxidation. *Environ. Pollut.* **2014**, *193*, 88−93.

(9) Zhang, R.; Khalizov, A.; Wang, L.; Hu, M.; Xu, W. Nucleation and Growth of Nanoparticles in the Atmosphere. *Chem. Rev.* **2012**, *112*, 1957−2011.

(10) Zhang, R.; Suh, I.; Zhao, J.; Zhang, D.; Fortner, E. C.; Tie, X.; Molina, L. T.; Molina, M. J. Atmospheric New Particle Formation Enhanced by Organic Acids. *Science* **2004**, *304*, 1487−1490.

(11) Jang, M.; Czoschke, N. M.; Lee, S.; Kamens, R. M. Heterogeneous Atmospheric Aerosol Production by Acid-Catalyzed Particle-Phase Reactions. *Science* **2002**, *298*, 814−817.

(12) Ding, X.; Wang, X.-M.; Zheng, M. The Influence of Temperature and Aerosol Acidity on Biogenic Secondary Organic Aerosol Tracers: Observations at a Rural Site in the Central Pearl River Delta Region, South China. *Atmos. Environ.* **2011**, *45*, 1303−1311.

(13) Claeys, M.; Graham, B.; Vas, G.; Wang, W.; Vermeylen, R.; Pashynska, V.; Cafmeyer, J.; Guyon, P.; Andreae, M. O.; Artaxo, P.;




DOI: 10.1021/acs.jpca.5b01321
J. Phys. Chem. A 2015, 119, 6583−6593

et al. Formation of Secondary Organic Aerosols through Photooxidation of Isoprene. *Science* **2004**, *303*, 1173−1176.
(14) Ng, N. L.; Kwan, A. J.; Surratt, J. D.; Chan, A. W. H.; Chhabra, P. S.; Sorooshian, A.; Pye, H. O. T.; Crounse, J. D.; Wennberg, P. O.; Flagan, R. C.; et al. Secondary Organic Aerosol (SOA) Formation from Reaction of Isoprene with Nitrate Radicals ($NO_3$). *Atmos. Chem. Phys.* **2008**, *8*, 4117−4140.
(15) Claeys, M.; Wang, W.; Ion, A. C.; Kourtchev, I.; Gelencsér, A.; Maenhaut, W. Formation of Secondary Organic Aerosols from Isoprene and Its Gas-Phase Oxidation Products through Reaction with Hydrogen Peroxide. *Atmos. Environ.* **2004**, *38*, 4093−4098.
(16) Carlton, A. G.; Wiedinmyer, C.; Kroll, J. H. A Review of Secondary Organic Aerosol (SOA) Formation from Isoprene. *Atmos. Chem. Phys.* **2009**, *9*, 4987−5005.
(17) Ng, N. L.; Chhabra, P. S.; Chan, A. W. H.; Surratt, J. D.; Kroll, J. H.; Kwan, A. J.; McCabe, D. C.; Wennberg, P. O.; Sorooshian, A.; Murphy, S. M.; et al. Effect of $NO_x$ Level on Secondary Organic Aerosol (SOA) Formation from the Photooxidation of Terpenes. *Atmos. Chem. Phys.* **2007**, *7*, 5159−5174.
(18) Docherty, K. S.; Wu, W.; Lim, Y. B.; Ziemann, P. J. Contributions of Organic Peroxides to Secondary Aerosol Formed from Reactions of Monoterpenes with $O_3$. *Environ. Sci. Technol.* **2005**, *39*, 4049−4059.
(19) Bonn, B.; Moortgat, G. K. Sesquiterpene Ozonolysis: Origin of Atmospheric New Particle Formation from Biogenic Hydrocarbons. *Geophys. Res. Lett.* **2003**, *30*, 1585.
(20) Vizuete, W.; Junquera, V.; Allen, D. T. Sesquiterpene Emissions and Secondary Organic Aerosol Formation Potentials for Southeast Texas. *Aerosol Sci. Technol.* **2004**, *38*, 167−181.
(21) Weber, R. J.; Sullivan, A. P.; Peltier, R. E.; Russell, A.; Yan, B.; Zheng, M.; de Gouw, J.; Warneke, C.; Brock, C.; Holloway, J. S.; et al. A Study of Secondary Organic Aerosol Formation in the Anthropogenic-Influenced Southeastern United States. *J. Geophys. Res.* **2007**, *112*, D13302.
(22) Volkamer, R.; Jimenez, J. L.; San Martini, F.; Dzepina, K.; Zhang, Q.; Salcedo, D.; Molina, L. T.; Worsnop, D. R.; Molina, M. J. Secondary Organic Aerosol Formation from Anthropogenic Air Pollution: Rapid and Higher Than Expected. *Geophys. Res. Lett.* **2006**, *33*, L17811.
(23) Nozière, B.; Kalberer, M.; Claeys, M.; Allan, J.; D'Anna, B.; Decesari, S.; Finessi, E.; Glasius, M.; Grgić, I.; Hamilton, J. F.; et al. The Molecular Identification of Organic Compounds in the Atmosphere: State of the Art and Challenges. *Chem. Rev.* **2015**, *115*, 3919−3983.
(24) Pratt, K. A.; Prather, K. A. Mass Spectrometry of Atmospheric Aerosols—Recent Developments and Applications. Part I: Off-Line Mass Spectrometry Techniques. *Mass. Spectrom. Rev.* **2012**, *31*, 1−16.
(25) Pratt, K. A.; Prather, K. A. Mass Spectrometry of Atmospheric Aerosols—Recent Developments and Applications. Part II: On-Line Mass Spectrometry Techniques. *Mass. Spectrom. Rev.* **2012**, *31*, 17−48.
(26) Hallquist, M.; Wenger, J. C.; Baltensperger, U.; Rudich, Y.; Simpson, D.; Claeys, M.; Dommen, J.; Donahue, N. M.; George, C.; Goldstein, A. H.; et al. The Formation, Properties and Impact of Secondary Organic Aerosol: Current and Emerging Issues. *Atmos. Chem. Phys.* **2009**, *9*, 5155−5236.
(27) Guenther, A.; Hewitt, C. N.; Erickson, D.; Fall, R.; Geron, C.; Graedel, T.; Harley, P.; Klinger, L.; Lerdau, M.; McKay, W. A.; et al. A Global Model of Natural Volatile Organic Compound Emissions. *J. Geophys. Res.* **1995**, *100*, 8873−8892.
(28) Zhang, D.; Zhang, R. Ozonolysis of $\alpha$-Pinene and $\beta$-Pinene: Kinetics and Mechanism. *J. Chem. Phys.* **2005**, *122*, 114308.
(29) Ma, Y.; Russell, A. T.; Marston, G. Mechanisms for the Formation of Secondary Organic Aerosol Components from the Gas-Phase Ozonolysis of $\alpha$-Pinene. *Phys. Chem. Chem. Phys.* **2008**, *10*, 4294−4312.
(30) Larsen, B. R.; Di Bella, D.; Glasius, M.; Winterhalter, R.; Jensen, N. R.; Hjorth, J. Gas-Phase OH Oxidation of Monoterpenes: Gaseous and Particulate Products. *J. Atmos. Chem.* **2001**, *38*, 231−276.
(31) Iinuma, Y.; Böge, O.; Gnauk, T.; Herrmann, H. Aerosol-Chamber Study of the $\alpha$-Pinene/$O_3$ Reaction: Influence of Particle Acidity on Aerosol Yields and Products. *Atmos. Environ.* **2004**, *38*, 761−773.
(32) Szmigielski, R.; Surratt, J. D.; Gómez-González, Y.; Van der Veken, P.; Kourtchev, I.; Vermeylen, R.; Blockhuys, F.; Jaoui, M.; Kleindienst, T. E.; Lewandowski, M., et al. 3-Methyl-1,2,3-Butanetricarboxylic Acid: An Atmospheric Tracer for Terpene Secondary Organic Aerosol. *Geophys. Res. Lett.* **2007**, *34*.
(33) Glasius, M.; Lahaniati, M.; Calogirou, A.; Di Bella, D.; Jensen, N. R.; Hjorth, J.; Kotzias, D.; Larsen, B. R. Carboxylic Acids in Secondary Aerosols from Oxidation of Cyclic Monoterpenes by Ozone. *Environ. Sci. Technol.* **2000**, *34*, 1001−1010.
(34) Glasius, M.; Duane, M.; Larsen, B. R. Determination of Polar Terpene Oxidation Products in Aerosols by Liquid Chromatography−Ion Trap Mass Spectrometry. *J. Chromatogr. A* **1999**, *833*, 121−135.
(35) Kleindienst, T. E.; Jaoui, M.; Lewandowski, M.; Offenberg, J. H.; Lewis, C. W.; Bhave, P. V.; Edney, E. O. Estimates of the Contributions of Biogenic and Anthropogenic Hydrocarbons to Secondary Organic Aerosol at a Southeastern US Location. *Atmos. Environ.* **2007**, *41*, 8288−8300.
(36) Ding, X.; Wang, X.-M.; Gao, B.; Fu, X.-X.; He, Q.-F.; Zhao, X.-Y.; Yu, J.-Z.; Zheng, M. Tracer-Based Estimation of Secondary Organic Carbon in the Pearl River Delta, South China. *J. Geophys. Res.* **2012**, *117*.
(37) Ding, X.; Wang, X.; Xie, Z.; Zhang, Z.; Sun, L. Impacts of Siberian Biomass Burning on Organic Aerosols over the North Pacific Ocean and the Arctic: Primary and Secondary Organic Tracers. *Environ. Sci. Technol.* **2013**, *47*, 3149−3157.
(38) Stone, E. A.; Hedman, C. J.; Zhou, J.; Mieritz, M.; Schauer, J. J. Insights into the Nature of Secondary Organic Aerosol in Mexico City During the Milagro Experiment 2006. *Atmos. Environ.* **2010**, *44*, 312−319.
(39) Jaoui, M.; Kleindienst, T. E.; Lewandowski, M.; Offenberg, J. H.; Edney, E. O. Identification and Quantification of Aerosol Polar Oxygenated Compounds Bearing Carboxylic or Hydroxyl Groups. 2. Organic Tracer Compounds from Monoterpenes. *Environ. Sci. Technol.* **2005**, *39*, 5661−5673.
(40) Praplan, A. P.; Barmet, P.; Dommen, J.; Baltensperger, U. Cyclobutyl Methyl Ketone as a Model Compound for Pinonic Acid to Elucidate Oxidation Mechanisms. *Atmos. Chem. Phys.* **2012**, *12*, 10749−10758.
(41) Salo, K.; Hallquist, M.; Jonsson, Å. M.; Saathoff, H.; Naumann, K. H.; Spindler, C.; Tillmann, R.; Fuchs, H.; Bohn, B.; Rubach, F.; et al. Volatility of Secondary Organic Aerosol During OH Radical Induced Ageing. *Atmos. Chem. Phys.* **2011**, *11*, 11055−11067.
(42) Zhang, Y. Y.; Müller, L.; Winterhalter, R.; Moortgat, G. K.; Hoffmann, T.; Pöschl, U. Seasonal Cycle and Temperature Dependence of Pinene Oxidation Products, Dicarboxylic Acids and Nitrophenols in Fine and Coarse Air Particulate Matter. *Atmos. Chem. Phys.* **2010**, *10*, 7859−7873.
(43) Qiu, C.; Zhang, R. Multiphase Chemistry of Atmospheric Amines. *Phys. Chem. Chem. Phys.* **2013**, *15*, 5738−5752.
(44) Zhang, R.; Wang, L.; Khalizov, A. F.; Zhao, J.; Zheng, J.; McGraw, R. L.; Molina, L. T. Formation of Nanoparticles of Blue Haze Enhanced by Anthropogenic Pollution. *Proc. Natl. Acad. Sci. U.S.A.* **2009**, *106*, 17650−17654.
(45) Bilde, M.; Pandis, S. N. Evaporation Rates and Vapor Pressures of Individual Aerosol Species Formed in the Atmospheric Oxidation of $\alpha$-and $\beta$-Pinene. *Environ. Sci. Technol.* **2001**, *35*, 3344−3349.
(46) Kroll, J. H.; Seinfeld, J. H. Chemistry of Secondary Organic Aerosol: Formation and Evolution of Low-Volatility Organics in the Atmosphere. *Atmos. Environ.* **2008**, *42*, 3593−3624.
(47) George, I. J.; Vlasenko, A.; Slowik, J. G.; Broekhuizen, K.; Abbatt, J. P. D. Heterogeneous Oxidation of Saturated Organic Aerosols by Hydroxyl Radicals: Uptake Kinetics, Condensed-Phase Products, and Particle Size Change. *Atmos. Chem. Phys.* **2007**, *7*, 4187−4201.


DOI: 10.1021/acs.jpca.5b01321
*J. Phys. Chem. A* 2015, 119, 6583−6593

(48) Kavouras, I. G.; Mihalopoulos, N.; Stephanou, E. G. Formation of Atmospheric Particles from Organic Acids Produced by Forests. *Nature* **1998**, *395*, 683−686.
(49) Cheng, Y.; Li, S.-M.; Leithead, A.; Brickell, P. C.; Leaitch, W. R. Characterizations of *cis*-Pinonic Acid and N-Fatty Acids on Fine Aerosols in the Lower Fraser Valley During Pacific 2001 Air Quality Study. *Atmos. Environ.* **2004**, *38*, 5789−5800.
(50) Liu, Y.; Liggio, J.; Harner, T.; Jantunen, L.; Shoeib, M.; Li, S. M. Heterogeneous OH Initiated Oxidation: A Possible Explanation for the Persistence of Organophosphate Flame Retardants in Air. *Environ. Sci. Technol.* **2014**, *48*, 1041−1048.
(51) Liu, Y.; Li, S. M.; Liggio, J. Application of Positive Matrix Factor Analysis in Heterogeneous Kinetics Studies: An Improvement to the Mixed-Phase Relative Rates Technique. *Atmos. Chem. Phys.* **2014**, *14*, 8695−8722.
(52) Liu, Y.; Huang, L.; Li, S. M.; Harner, T.; Liggio, J. OH-Initiated Heterogeneous Oxidation of tris-2-Butoxyethyl Phosphate: Implications for Its Fate in the Atmosphere. *Atmos. Chem. Phys.* **2014**, *14*, 12195−12207.
(53) Lai, C.; Liu, Y.; Ma, J.; Ma, Q.; He, H. Degradation Kinetics of Levoglucosan Initiated by Hydroxyl Radical under Different Environmental Conditions. *Atmos. Environ.* **2014**, *91*, 32−39.
(54) Pietrogrande, M. C.; Bacco, D.; Mercuriali, M. GC-MS Analysis of Low-Molecular-Weight Dicarboxylic Acids in Atmospheric Aerosol: Comparison between Silylation and Esterification Derivatization Procedures. *Anal. Bioanal. Chem.* **2010**, *396*, 877−885.
(55) Chiueh, C. C.; Krishna, G.; Tulsi, P.; Obata, T.; Lang, K.; Huang, S.-J.; Murphy, D. L. Intracranial Microdialysis of Salicylic Acid to Detect Hydroxyl Radical Generation through Dopamine Autooxidation in the Caudate Nucleus: Effects of Mpp+. *Free. Radical. Bio. Med.* **1992**, *13*, 581−583.
(56) Hennigan, C. J.; Sullivan, A. P.; Collett, J. L.; Robinson, A. L. Levoglucosan Stability in Biomass Burning Particles Exposed to Hydroxyl Radicals. *Geophys. Res. Lett.* **2010**, *37*, L09806.
(57) Frisch, M. J.; Trucks, G. W.; Schlegel, H. B.; Scuseria, G. E.; Robb, M. A.; Cheeseman, J. R. G.; Calmani, V.; Barone, B.; Mennucci, G. A.; Petersson, H., et al. Gaussian 09, Gaussian. Inc.: Wallingford, CT, 2009.
(58) Merrick, J. P.; Moran, D.; Radom, L. An Evaluation of Harmonic Vibrational Frequency Scale Factors. *J. Phys. Chem. A* **2007**, *111*, 11683−11700.
(59) Berndt, T.; Richters, S. Products of the Reaction of OH Radicals with Dimethyl Sulphide in the Absence of $NO_x$: Experiment and Simulation. *Atmos. Environ.* **2012**, *47*, 316−322.
(60) Coeur-Tourneur, C.; Foulon, V.; Laréal, M. Determination of Aerosol Yields from 3-Methylcatechol and 4-Methylcatechol Ozonolysis in a Simulation Chamber. *Atmos. Environ.* **2010**, *44*, 852−857.
(61) Keyser, L. F.; Moore, S. B.; Leu, M. T. Surface Reaction and Pore Diffusion in Flow-Tube Reactors. *J. Phys. Chem.* **1991**, *95*, 5496−5502.
(62) Underwood, G. M.; Li, P.; Al-Abadleh, H.; Grassian, V. H. A Knudsen Cell Study of the Heterogeneous Reactivity of Nitric Acid on Oxide and Mineral Dust Particles. *J. Phys. Chem. A* **2001**, *105*, 6609−6620.
(63) Widmann, J. F.; Davis, E. J. Mathematical Models of the Uptake of $ClONO_2$ and Other Gases by Atmospheric Aerosols. *J. Aerosol Sci.* **1997**, *28*, 87−106.
(64) George, I. J.; Abbatt, J. P. Heterogeneous Oxidation of Atmospheric Aerosol Particles by Gas-Phase Radicals. *Nat. Chem.* **2010**, *2*, 713−722.
(65) Atkinson, R. Kinetics and Mechanisms of the Gas-Phase Reactions of the Hydroxyl Radical with Organic-Compounds under Atmospheric Conditions. *Chem. Rev.* **1985**, *85*, 69−201.
(66) Atkinson, R.; Arey, J. Atmospheric Degradation of Volatile Organic Compounds. *Chem. Rev.* **2003**, *103*, 4605−4638.
(67) Vereecken, L.; Peeters, J. Enhanced H-Atom Abstraction from Pinonaldehyde, Pinonic Acid, Pinic Acid, and Related Compounds: Theoretical Study of C-H Bond Strengths. *Phys. Chem. Chem. Phys.* **2002**, *4*, 467−472.
(68) Lee, W.; Stevens, P. S.; Hites, R. A. Rate Constants for the Gas-Phase Reactions of Methylphenanthrenes with OH as a Function of Temperature. *J. Phys. Chem. A* **2003**, *107*, 6603−6608.
(69) Perry, R. A.; Atkinson, R.; Pitts, J. N. Kinetics and Mechanism of the Gas Phase Reaction of Hydroxyl Radicals with Aromatic Hydrocarbons over the Temperature Range 296−473 K. *J. Phys. Chem.* **1977**, *81*, 296−304.
(70) Mochida, M.; Kawamura, K.; Fu, P.; Takemura, T. Seasonal Variation of Levoglucosan in Aerosols over the Western North Pacific and Its Assessment as a Biomass-Burning Tracer. *Atmos. Environ.* **2010**, *44*, 3511−3518.
(71) Hoffmann, D.; Tilgner, A.; Iinuma, Y.; Herrmann, H. Atmospheric Stability of Levoglucosan - a Detailed Laboratory and Modeling Study. *Environ. Sci. Technol.* **2010**, *44*, 694−699.
(72) Ma, Q.; Liu, Y.; He, H. The Utilization of Physisorption Analyzer for Studying the Hygroscopic Properties of Atmospheric Relevant Particles. *J. Phys. Chem. A* **2010**, *114*, 4232−4237.
(73) Chan, L. P.; Chan, C. K. Displacement of Ammonium from Aerosol Particles by Uptake of Triethylamine. *Aerosol Sci. Technol.* **2012**, *46*, 236−247.
(74) Kuwata, M.; Martin, S. T. Phase of Atmospheric Secondary Organic Material Affects Its Reactivity. *Proc. Natl. Acad. Sci. U.S.A.* **2012**, *109*, 17354−17359.
(75) Slade, J. H.; Knopf, D. A. Multiphase OH Oxidation Kinetics of Organic Aerosol: The Role of Particle Phase State and Relative Humidity. *Geophys. Res. Lett.* **2014**, *41*, 5297−5306.
(76) Ataol, Ç. Y.; Ekici, Ö. Experimental and Theoretical Studies of (FTIR, FT-NMR, UV−Visible, X-Ray and DFT) 2-(4-Allyl-5-pyridin-4-yl-4*h*-[1,2,4]triazol-3-ylsulfanyl)-1-(3-methyl-3-phenyl-cyclobutyl)-ethanone. *J. Mol. Struct.* **2014**, *1065−1066*, 1−9.
(77) Lin, S.-Y.; Chen, K.-S.; Liang, R.-C. Thermal Micro ATR/FT-IR Spectroscopic System for Quantitative Study of the Molecular Structure of Poly(*N*-Isopropylacrylamide) in Water. *Polymer* **1999**, *40*, 2619−2624.
(78) Lu, R.; Gan, W.; Wu, B.; Chen, H.; Wang, H. Vibrational Polarization Spectroscopy of CH Stretching Modes of the Methylene Group at the Vapor/Liquid Interfaces with Sum Frequency Generation. *J. Phys. Chem. B* **2004**, *108*, 7297−7306.
(79) Gómez-Serrano, V.; Piriz-Almeida, F.; Durán-Valle, C. J.; Pastor-Villegas, J. Formation of Oxygen Structures by Air Activation. A Study by FT-IR Spectroscopy. *Carbon* **1999**, *37*, 1517−1528.
(80) Ibrahim, M.; Nada, A.; Kamal, D. E. Density Functional Theory and FTIR Spectroscopic Study of Carboxyl Group. *Indian J. Pure Appl. Phys.* **2005**, *43*, 911−917.
(81) Kourtchev, I.; Hellebust, S.; Bell, J. M.; O'Connor, I. P.; Healy, R. M.; Allanic, A.; Healy, D.; Wenger, J. C.; Sodeau, J. R. The Use of Polar Organic Compounds to Estimate the Contribution of Domestic Solid Fuel Combustion and Biogenic Sources to Ambient Levels of Organic Carbon and $PM_{2.5}$ in Cork Harbour, Ireland. *Sci. Total Environ.* **2011**, *409*, 2143−2155.
(82) Atkinson, R. Estimation of Gas-Phase Hydroxyl Radical Rate Constants for Organic Chemicals. *Environ. Toxicol. Chem.* **1988**, *7*, 435−442.
(83) Kwok, E. S. C.; Atkinson, R. Estimation of Hydroxyl Radical Reaction-Rate Constants for Gas-Phase Organic-Compounds Using a Structure-Reactivity Relationship - an Update. *Atmos. Environ.* **1995**, *29*, 1685−1695.
(84) Prinn, R. G.; Huang, J.; Weiss, R. F.; Cunnold, D. M.; Fraser, P. J.; Simmonds, P. G.; McCulloch, A.; Harth, C.; Salameh, P.; O'Doherty, S.; et al. Evidence for Substantial Variations of Atmospheric Hydroxyl Radicals in the Past Two Decades. *Science* **2001**, *292*, 1882−1888.
(85) Prinn, R. G.; Huang, J.; Weiss, R. F.; Cunnold, D. M.; Fraser, P. J.; Simmonds, P. G.; McCulloch, A.; Harth, C.; Reimann, S.; Salameh, P.; et al. Evidence for Variability of Atmospheric Hydroxyl Radicals over the Past Quarter Century. *Geophys. Res. Lett.* **2005**, *32*, L07809.
(86) Tkacik, D. S.; Lambe, A. T.; Jathar, S.; Li, X.; Presto, A. A.; Zhao, Y.; Blake, D.; Meinardi, S.; Jayne, J. T.; Croteau, P. L.; et al. Secondary Organic Aerosol Formation from in-Use Motor Vehicle


DOI: 10.1021/acs.jpca.5b01321
*J. Phys. Chem. A* 2015, 119, 6583−6593

Emissions Using a Potential Aerosol Mass Reactor. *Environ. Sci. Technol.* **2014**, *48*, 11235−11242.
(87) Zhou, S.; Lee, A. K. Y.; McWhinney, R. D.; Abbatt, J. P. D. Burial Effects of Organic Coatings on the Heterogeneous Reactivity of Particle-Borne Benzo[*a*]pyrene (BaP) toward Ozone. *J. Phys. Chem. A* **2012**, *116*, 7050−7056.
(88) Badger, C. L.; Griffiths, P. T.; George, I.; Abbatt, J. P.; Cox, R. A. Reactive Uptake of $N_2O_5$ by Aerosol Particles Containing Mixtures of Humic Acid and Ammonium Sulfate. *J. Phys. Chem. A* **2006**, *110*, 6986−6994.



DOI: 10.1021/acs.jpca.5b01321
*J. Phys. Chem. A* 2015, 119, 6583−6593